A comparison of electrochemical oxidation performance of PbO_2 and SnO_2 electrodes

X. Y. Duan, J. R. Li, L. M. Chang and C. W. Yang

ABSTRACT

PbO_2 and SnO_2 are two promising anode materials for electrochemical oxidation. In order to highlight the difference between two kinds of electrodes in an electrochemical oxidation process, their morphology, structural, oxygen evolution overpotential (OEP), electrochemical activity and service life-time were compared in detail in this paper. Surface characterization by scanning electron microscope shows that the film of the PbO_2 electrode is even, compact, non-porous, and non-cracked, while many cracks are present on the film of the SnO_2 electrode. Electrochemical studies based on linear sweep voltammetry (LSV) and cyclic voltammetry (CV) prove that the OEP for the SnO_2 electrode was much higher than that of the PbO_2 electrode, and the electron-transfer kinetics and the reversibility of electrode reaction of the SnO_2 electrode were superior to those of the PbO_2 electrode. In electrochemical decomposition of *p*-nitrophenol, the degradation ratios at PbO_2 and SnO_2 anodes achieved 86.9% and 96.5%, respectively, after 120 min electrolysis, which verified the results of LSV and CV. The accelerated lifetime tests show that the service life time of the SnO_2 electrode is far shorter than that of the PbO_2 electrode, even though it was shown to be superior to the PbO_2 in electrocatalytic activity.

Key words | comparison, electrochemical oxidation, electrode, PbO_2, SnO_2

X. Y. Duan (corresponding author)
C. W. Yang
School of Environmental Science and Engineering,
Jilin Normal University,
Siping 136000,
China
E-mail: *duanxiaoyue0511@163.com*

J. R. Li
L. M. Chang
Key Laboratory of Preparation and Applications of Environmental Friendly Materials,
Jilin Normal University,
Ministry of Education,
Changchun 130103,
China

INTRODUCTION

Fresh water scarcity has been a severe problem in recent years. Moreover, an increase in water pollutant levels is directly threatening the safety of drinking water for humans and animals. Thus, extensive wastewater treatment technologies have been developed, among which electrochemical oxidation is a promising approach for the degradation of refractory organic pollutants in water due to its many distinctive advantages including strong oxidation performance, environmental compatibility, versatility, cost effectiveness and amenability to automation (Zhuo *et al.* 2011; Liu *et al.* 2012).

The degradation efficiency of organic pollutants in an electrochemical oxidation process depends on the activity of the anode materials (Zhao *et al.* 2014). Besides high activity, high chemical stability is one of the basic features for the optimal electrode. Typical anode materials include graphite (Chen *et al.* 2010), Pt (Torres *et al.* 2005), activated carbon fiber (Yi *et al.* 2008), boron-doped diamond (Nasr & Abdelatif 2009), PbO_2 (Wang *et al.* 2010), SnO_2 (Río *et al.* 2010), IrO_2 (Tolba *et al.* 2010), RuO_2 (Tran *et al.* 2009) and MnO_2 (Lin *et al.* 2012). Among all these anode materials, PbO_2 and SnO_2 are two promising candidates in view of their effective degradation for organic pollutants, simple preparation process and low cost. In previous studies, the degradation applications of a variety of organic wastewaters were reported for these two electrodes, such as dye wastewater (Río *et al.* 2010), landfill leachate (Panizza & Martinez-Huitle 2013), carwash wastewater (Panizza & Cerisola 2010), tannery wastewater (Costa *et al.* 2008), and various toxic organics (Samet *et al.* 2010; Zhu *et al.* 2010; Hamza *et al.* 2011). Thus, in this paper, PbO_2 and SnO_2 electrodes were prepared and their electro-catalytic

doi: 10.2166/wrd.2016.150

characterizations were analyzed and compared by scanning electron microscopy (SEM), X-ray diffraction (XRD), linear sweep voltammetry (LSV), cyclic voltammetry (CV), and electrochemical degradation of *p*-nitrophenol (*p*-NP). Also, the service life of PbO_2 and SnO_2 electrodes was determined by accelerated life tests.

METHODS

Electrode preparation

The PbO_2 electrode was prepared by electro-deposition. The specific details of the preparation method can be found in Duan *et al.* (2013).

The SnO_2 electrode was prepared by thermal deposition. Firstly, Ti substrates underwent a preparation of sandblasting, 10 min of ultrasonic cleaning in acetone, 10 min of ultrasonic cleaning in deionized water, 2 h of etching in boiling aqueous 15% oxalic acid, and rinsing with deionized water. Then, the pretreated Ti substrates were brushed with a solution containing 20 g $SnCl_4{\cdot}5H_2O$ and 2 g $SbCl_3$ in 100 mL of isopropanol-HCl mixture, dried at 120 °C for 10 min, and baked at 500 °C for 10 min. This procedure was repeated 10 times. Finally, the Ti substrate was annealed at 500 °C for 1 h.

Electrode characterization

SEM was carried out on a Hitachi S-570 model instrument. XRD patterns of samples were obtained with an XRD (Rigaku D-max/3C) using Cu Kα radiation (45 kV, 30 mA). LSV and CV were executed in the PGSTAT302 electrochemical workstation. LSV and CV measurements were both carried out with a conventional three-electrode system. The fabricated PbO_2 and SnO_2 electrodes were used as the working electrode, a platinum sheet as the auxiliary electrode, and a saturated calomel electrode as the reference electrode.

Batch experiment

The electrochemical degradation experiments of *p*-NP were carried out by batch processes and the apparatus mainly consisted of a direct-current power supply, a heat-gathering style magnetic stirrer and a glass reactor. The anode (PbO_2 or SnO_2 electrode) and cathode (stainless steel sheet) were positioned vertically and parallel to each other at a distance of 1 cm. The initial concentration of *p*-NP during all the experimental runs was 50 mg L^{-1} of a volume of 200 mL; 0.05 M Na_2SO_4 was used as the supporting electrolyte. The reaction temperature was kept at 30 °C during all the experimental runs. Electrochemical degradation was performed at a current density of 30 mA cm^{-2}. During the experiments, samples were drawn from the reactor at certain intervals and then analyzed. The disappearance of *p*-NP during electrolysis was analyzed using a spectrophotometric technique ($\lambda = 273$ nm).

Electrode stability

Stability tests for the electrodes were carried out in a three electrode cell in 2 M H_2SO_4 solution at 60 °C with a constant anodic current density of 1 A cm^{-2}. The fabricated PbO_2 or SnO_2 electrodes were used as the anode, a stainless steel sheet as the cathode, and a saturated Ag/AgCl as the reference electrode. The anode potential was periodically monitored with time. The service lifetime of an electrode is defined as the operation time at which the anodic potential increased rapidly by 5 V (vs. Ag/AgCl).

RESULTS AND DISCUSSION

Surface morphology and phase structure

The SEM images of PbO_2 and SnO_2 electrodes are shown in Figure 1. The PbO_2 electrode (Figure 1(a)) consists of a large number of typical pyramid-structure crystal particles. The film of the PbO_2 electrode is even, compact, non-porous, and non-cracked. However, the SnO_2 electrode presents a 'mud crack' morphology (Figure 1(b)), which was a specific feature of thermal deposition. In addition, there are many cracks on the film of the SnO_2 electrode, which was a result of mechanism tension caused by the plasticity of the coating and the difference of the thermal expansion coefficient between the base metal and the coating (Comninellis & Vercesi 1991; Wang *et al.* 2010).

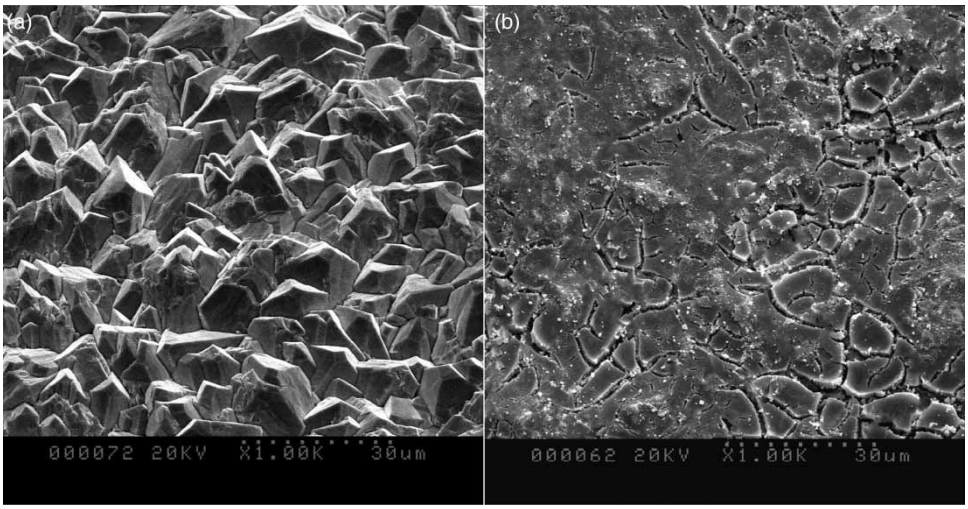

Figure 1 | SEM images of a PbO_2 electrode (a) and an SnO_2 electrode (b).

Figure 2 presents the XRD patterns of PbO_2 and SnO_2 electrodes. The XRD pattern of the PbO_2 electrode presents diffraction peaks of pure β-PbO_2. However, from the XRD pattern of the SnO_2 electrode, two kinds of crystalline structures including SnO_2 and Ti are observed. The presence of diffraction peaks of Ti demonstrates that the formed SnO_2 film was still so thin that the X-ray went to the Ti substrate. In addition, it can be found that no diffraction peak of Sb_2O_3 was observed in the pattern of the SnO_2 electrode because there was too little Sb dopant in the film to be detected by XRD analysis.

Electrochemical measurements

The oxygen evolution overpotential (OEP) of the PbO_2 and SnO_2 electrodes was measured by means of LSV in 0.5 M Na_2SO_4 solution at a scan rate of 50 mV s^{-1}, and the potential corresponding to the inflection point of the polarization curve was defined as the OEP of the electrode. Figure 3 represents typical polarization curves for two kinds of electrodes. According to the polarization curves, the OEP for the PbO_2 electrode is approximately 1.55 V (vs. SCE), while the OEP value on the SnO_2 electrode is 1.85 V (vs. SCE), much higher than that of the PbO_2 electrode. The

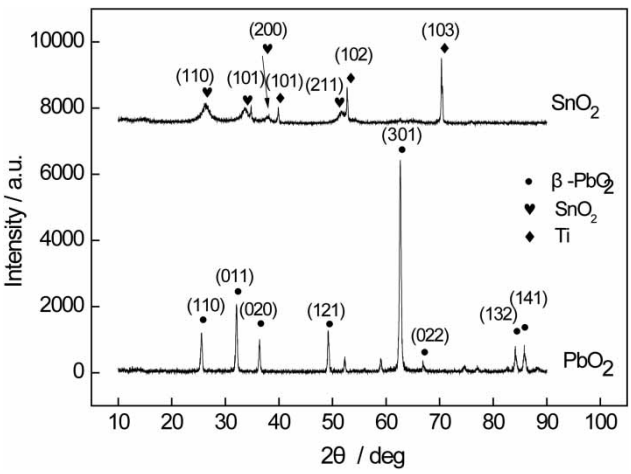

Figure 2 | XRD patterns of PbO_2 and SnO_2 electrodes.

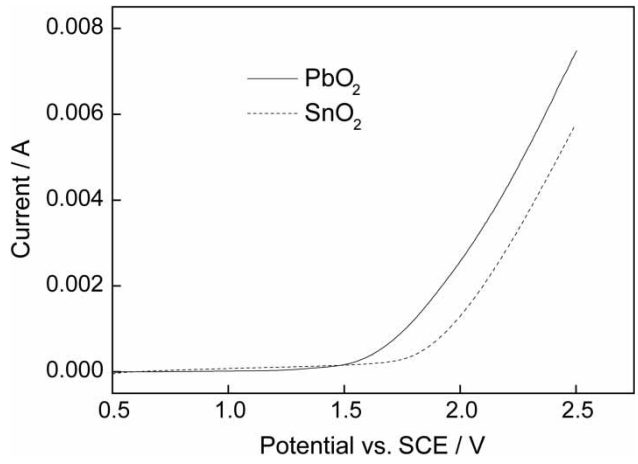

Figure 3 | LSV curves of different electrodes measured in 0.5 M Na_2SO_4 solution at 25 °C, scan rate: 10 mV s^{-1}.

higher OEP of the SnO_2 electrode indicates that the SnO_2 electrode should have better electrocatalytic activity and degradation performance for organic pollutants in the electro-catalytic oxidation process (Amadelli *et al.* 2002; Yao *et al.* 2014). However, this result is not in agreement with the previous reports for the OEP on Pb/PbO_2 and Ti/SnO_2 anodes, in which Pb/PbO_2 material presented higher OEP than Ti/SnO_2 material (Vazquez-Gomez *et al.* 2012). This conflict may be attributed to the difference in the preparation processes of the electrodes.

The CV measurements in 1.0 M KCl solution containing 5.0 mM $K_3Fe(CN)_6$ and 5.0 mM $K_4Fe(CN)_6$ were conducted to estimate the electrochemical activity of PbO_2 and SnO_2 electrodes. Figure 4(a) and 4(b) shows the CV curves recorded

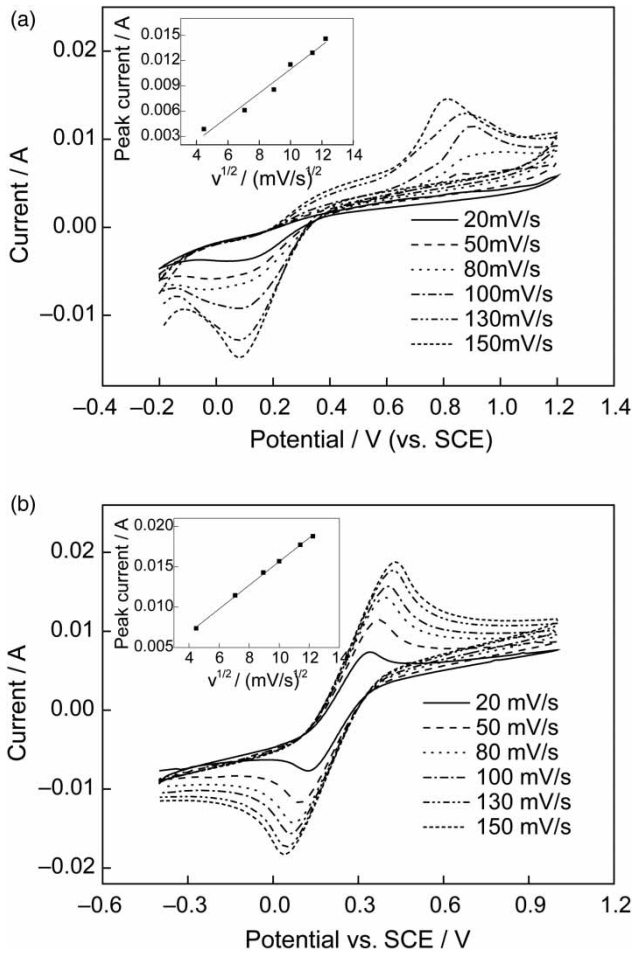

Figure 4 | Cyclic voltammograms of PbO_2 (a) and SnO_2 (b) electrodes in 1.0 mol L^{-1} KCl containing 5.0 mmol L^{-1} $K_3Fe(CN)_6$ and 5.0 mmol L^{-1} $K_4Fe(CN)_6$. Insets show the plots of peak current versus the square root of scan rate.

for the PbO_2 and SnO_2 electrodes, respectively, at scan rates of 20 mV s^{-1}, 50 mV s^{-1}, 80 mV s^{-1}, 100 mV s^{-1}, 130 mV s^{-1}, and 150 mV s^{-1}. There are a pair of distinct anodic and cathodic peaks observed for two kinds of electrodes corresponding to the redox reactions through a direct electron-transfer process between $Fe(CN)_6^{4-}$ and $Fe(CN)_6^{3-}$ at all scans. Comparing two sets of CV curves, it also can be found that sharper, larger and narrower redox peaks appeared on the CV curves of the SnO_2 electrode. Besides, the peak potential separation (ΔE_p) for the SnO_2 electrode was significantly smaller than that of the PbO_2 electrode. For example, at a scan rate of 100 mV s^{-1}, the ΔE_p values were 356 mV and 823 mV for the SnO_2 and PbO_2 electrodes, respectively. All these results suggest that the electron-transfer kinetics and the reversibility of the electrode reaction of the SnO_2 electrode were superior to those of the PbO_2 electrode.

CV measurements were also performed in 0.5 M Na_2SO_4 solution containing 200 mg L^{-1} *p*-NP to investigate the direct electrochemical oxidation performance of the PbO_2 and SnO_2 electrodes. The cyclic voltammograms are shown in Figure 5(a) and 5(b). For comparison, the cyclic voltammograms in blank Na_2SO_4 solution are also shown in Figure 5(c) and 5(d).

From the curves of the PbO_2 electrode (Figure 5(a) and 5(c)), it can be observed that there were three oxidation peaks in the anodic branches and one reduction peak in the cathodic branch with and without the presence of *p*-NP. Interestingly, the current response of the third oxidation peak (at about 1.2 V vs. SCE) with *p*-NP is much higher than that without *p*-NP in the first cycle, but in the subsequent cycles, if *p*-NP existed in the solution, this peak decreased to total disappearance, if not, it increased slowly and moved negatively. These differences indicate that the third oxidation peak in Figure 5(a) should be attributed to the oxidation reaction of *p*-NP on the surface of the PbO_2 electrode, which may overlap the oxidation peak of formation of PbO_2 in Figure 5(c). The gradual disappearance of peaks in Figure 5(a) with the increase in scan times means that a passivation film was formed on the surface of the PbO_2 electrode during the oxidation of *p*-NP in Na_2SO_4 solution, which prevented all reactions further occurring on the surface of the electrode.

In the voltammogram of the SnO_2 electrode in Na_2SO_4 solution containing *p*-NP (Figure 5(b)), an irreversible oxidation peak presented at 1.25 V vs. SCE in the first cycle.

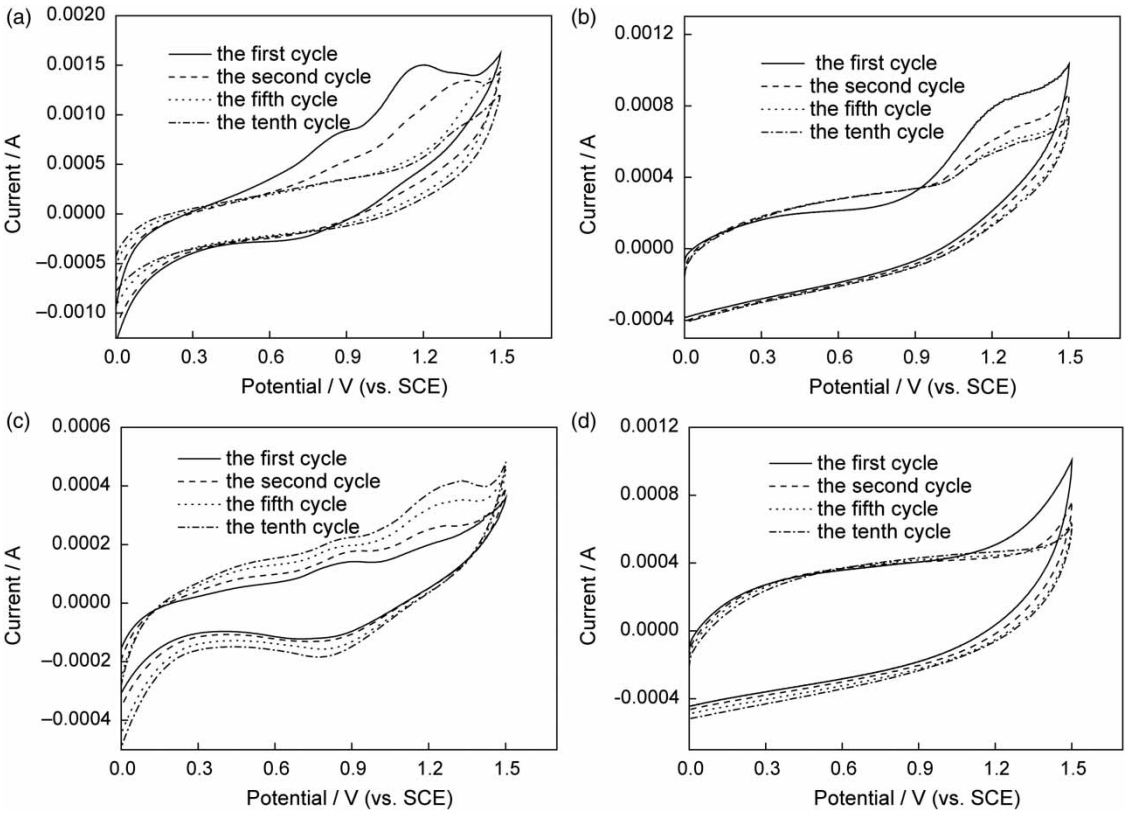

Figure 5 | Cyclic voltammograms of the PbO_2 ((a) and (c)) and SnO_2 ((b) and (d)) electrodes in 1 mol L^{-1} Na_2SO_4 solution with and without 500 mg L^{-1} *p*-NP. Scan rate: 50 mV s^{-1}.

Compared with that in blank Na_2SO_4 solution (Figure 5(d)), it can be determined that this oxidation peak was ascribed to the oxidation of *p*-NP on the surface of the SnO_2 electrode. It can also be observed that, in subsequent cycles, the oxidation peak decreased gradually during the successive cyclic voltammetric sweeps, but it still exists until the tenth cycle, which shows that passivation also occurred on the SnO_2 electrode, but the rate of passivation was slower than that of the PbO_2 electrode.

Degradation of *p*-NP on different electrodes

Electrochemical degradation experiments of *p*-NP at PbO_2 and SnO_2 anodes were performed by applying 30 mA cm^{-2} of current density. Figure 6(a) demonstrates the *p*-NP removal percentage variation by utilizing PbO_2 and SnO_2 as anodes during the electrochemical oxidation process. It can be observed that *p*-NP could be degraded on these two anodes and the *p*-NP removal percentages for both electrodes increased with the increase in reaction time. However, it is also worth noting that the degradation rates of *p*-NP varied according to the type of anode. At the SnO_2 electrode, the removal percentage was 96.5% after 2 h. However, at the PbO_2 anode, the corresponding removal percentage was 86.9%, a lower value than that obtained at the SnO_2 electrode. The plots of $\ln(C_0/C)$ versus time are shown in Figure 6(b). The linear relationships manifest the electrochemical oxidation of *p*-NP via a pseudo-first-order mechanism, with rate constants of 0.0174 min^{-1} at the PbO_2 electrode and 0.0285 min^{-1} at the SnO_2 electrode. Thus, we can conclude that the SnO_2 electrode had a stronger oxidation performance for *p*-NP, which was in agreement with the above deduction in polarization curves.

Electrode stability

Figure 7 compares the stability of the PbO_2 and SnO_2 electrodes by accelerated life tests. As seen in Figure 7,

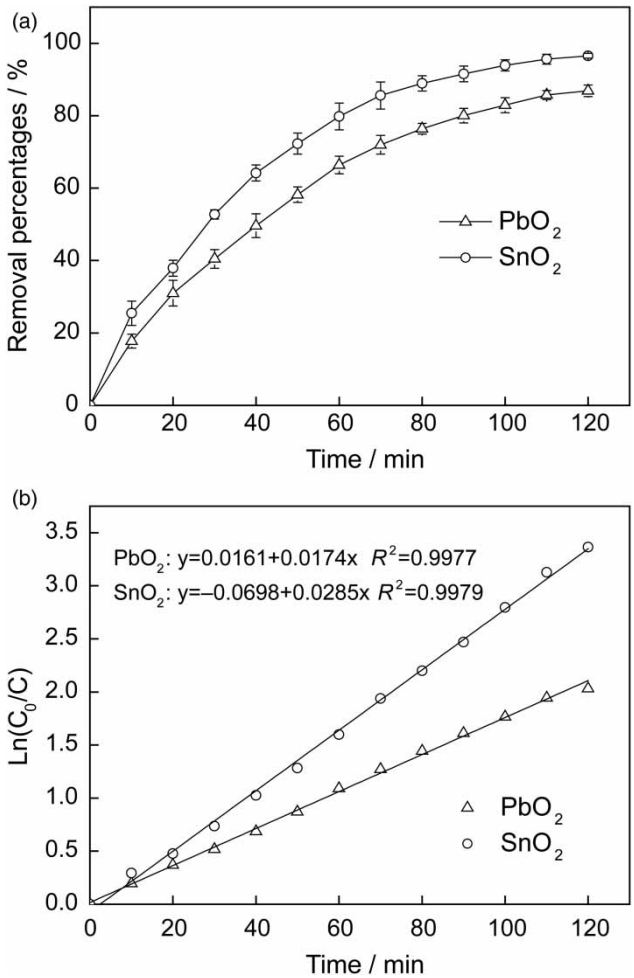

Figure 6 | Variation of *p*-NP removal percentage with time during electrochemical oxidation (a) and pseudo-first-order kinetics fitting curves (b) on PbO_2 and SnO_2 electrodes. Conditions: current density = 50 mA cm^{-2}; T = 30 °C; [*p*-NP] = 50 mg L^{-1}; [Na_2SO_4] = 0.05 mol L^{-1}.

the PbO_2 electrode had a service life of 56 h, which was 37 times longer than that of the SnO_2 electrode. This is attributed to the different morphologies of PbO_2 and SnO_2 electrodes. The PbO_2 electrode was prepared by electrodeposition, as shown in Figure 1, its film was compact, non-porous, and non-cracked, which not only reduced the penetration of electrolyte through cracks or pores (Yao *et al.* 2014), but also suppressed the formation of TiO_2 on the Ti substrate and internal O_2 evolution under the film. On the contrary, the electrolyte easily penetrated the cracks on the SnO_2 electrode, leading to the breaking off of the coating.

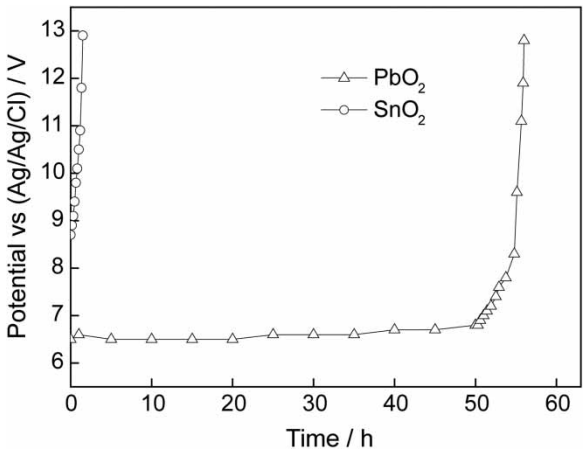

Figure 7 | Electrode stability tests: electrode potential (vs. Ag/AgCl) vs. time for the electrolysis (1 A cm^{-2}, 60 °C) in 2 mol L^{-1} H_2SO_4 using PbO_2 and SnO_2 electrodes as anodes.

CONCLUSIONS

In this work, the electro-catalytic activities and service lifetime of PbO_2 and SnO_2 electrodes were compared in detail for the electrochemical oxidation process. The main conclusions are as follows: the film of the PbO_2 electrode is even, compact, non-porous, and non-cracked, while there were many cracks present on the film of the SnO_2 electrode. LSV proves that the OEP for the SnO_2 electrode is much higher than that of the PbO_2 electrode. The electron-transfer kinetics and the reversibility of the electrode reaction of the SnO_2 electrode were superior to those of the PbO_2 electrode in CV measurements. The results of bulk electrolysis show that *p*-NP can be readily degraded at PbO_2 and SnO_2 anodes, and the decay kinetics of *p*-NP on both anodes follow a pseudo-first-order reaction. Although high over voltage anode material SnO_2 was shown to be superior to the PbO_2, a comparison of service lifetime of the two electrode materials showed that the PbO_2 electrode had a service life of 56 h, which is 37 times longer than that of the SnO_2 electrode.

ACKNOWLEDGEMENTS

This project was supported financially by the Young People Fund (20150520079JH) and Natural Science Fund (20140101215JC) of the Jilin Science and Technology

Department, China. This work was also supported by the Development Program (2014055) of the Siping Technology Bureau, China.

REFERENCES

Amadelli, R., Maldotti, A., Molinari, A., Danilov, F. I. & Velichenko, A. B. 2002 Influence of the electrode history and effects of the electrolyte composition and temperature on O_2 evolution at β-PbO_2 anodes in acid media. *J. Electroanal. Chem.* **534** (1), 1–12.

Chen, J. L., Chiou, G. C. & Wu, C. C. 2010 Electrochemical oxidation of 4-chlorophenol with granular graphite electrodes. *Desalination* **264** (1–2), 92–96.

Comninellis, C. H. & Vercesi, G. P. 1991 Characterization of DSA-type oxygen evolving electrodes: choice of a coating. *J. Appl. Electrochem.* **21** (4), 335–345.

Costa, C. R., Botta, C. M. R., Espindola, E. L. G. & Qlivi, P. 2008 Electrochemical treatment of tannery wastewater using DSA electrodes. *J. Hazard. Mater.* **153** (1–2), 616–627.

Duan, X., Ma, F., Yuan, Z., Chang, L. & Jin, X. 2013 Electrochemical degradation of phenol in aqueous solution using PbO_2 anode. *J. Taiwan Inst. Chem. E.* **44** (1), 95–102.

Hamza, M., Ammar, S. & Abdelhédi, R. 2011 Electrochemical oxidation of 1,3,5-trimethoxybenzene in aqueous solution at gold and lead dioxide electrodes. *Electrochim. Acta* **56** (11), 3785–3789.

Lin, H., Niu, J., Ding, S. & Zhang, L. 2012 Electrochemical degradation of perfluorooctanoic acid (PFOA) by Ti/SnO_2-Sb, Ti/SnO_2-Sb/PbO_2 and Ti/SnO_2-Sb/MnO_2 anodes. *Water Res.* **46** (7), 2281–2289.

Liu, Y., Liu, H., Ma, J. & Li, J. 2012 Preparation and electrochemical properties of Ce-Ru-SnO_2 ternary oxide anode and electrochemical oxidation of nitrophenols. *J. Hazard. Mater.* **213–214** (7), 222–229.

Nasr, B. & Abdelatif, G. 2009 Electrochemical treatment of wastewaters containing 4-chlororesorcinol using boron doped diamond anodes. *Can. J. Chem. Eng.* **87** (1), 78–84.

Panizza, M. & Cerisola, G. 2010 Applicability of electrochemical methods to carwash wastewater for reuse. Part 1: anodic oxidation with diamond and lead dioxide anodes. *J. Electroanal. Chem.* **638** (1), 28–32.

Panizza, M. & Martinez-Huitle, C. A. 2013 Role of electrode materials for the anodic oxidation of a real landfill leachate – comparison between Ti-Ru-Sn ternary oxide, PbO_2 and boron-doped diamond anode. *Chemosphere* **90** (4), 1455–1460.

Río, A. I., Fernández, J., Molina, J., Bonastre, J. & Cases, F. 2010 On the behaviour of doped SnO_2 anodes stabilized with platinum in the electrochemical degradation of reactive dyes. *Electrochim. Acta* **55** (24), 7282–7289.

Samet, Y., Agengui, L. & Abdelhédi, R. 2010 Anodic oxidation of chlorpyrifos in aqueous solution at lead dioxide electrodes. *J. Electroanal. Chem.* **650** (1), 152–158.

Tolba, R., Tian, M., Wen, J., Jiang, Z. H. & Chen, A. 2010 Electrochemical oxidation of lignin at IrO_2-based oxide electrodes. *J. Electroanal. Chem.* **649** (1–2), 9–15.

Torres, R. A., Torres, W., Peringer, P. & Pulgarin, C. 2003 Electrochemical degradation of *p*-substituted phenols of industrial interest on Pt electrodes. Attempt of a structure-reactivity relationship assessment. *Chemosphere* **50** (1), 97–104.

Tran, L. H., Drogui, P., Mercier, G. & Blais, J. F. 2009 Electrochemical degradation of polycyclic aromatic hydrocarbons in creosote solution using ruthenium oxide on titanium expanded mesh anode. *J. Hazard. Mater.* **164** (2–3), 1118–1129.

Vazquez-Gomez, L., Battisti, A., Ferro, S., Cerro, M., Reyna, S., Martínez-Huitle, C. A. & Quiroz, M. A. 2012 Anodic oxidation as green alternative for removing diethyl phthalate from wastewater using Pb/PbO_2 and Ti/SnO_2 anodes. *Clean-Soil Air Water* **40** (4), 408–415.

Wang, Y., Shen, Z., Li, Y. & Niu, J. 2010 Electrochemical properties of the erbium-chitosan-modified PbO_2 electrode for the degradation of 2,4-dichlorophenol in aqueous solution. *Chemosphere* **79** (10), 987–996.

Yao, Y., Zhao, M., Zhao, C. & Zhang, H. 2014 Preparation and properties of PbO_2-ZrO_2 nanocomposite electrodes by pulse electrodeposition. *Electrochim. Acta* **117** (2), 453–459.

Yi, F., Chen, S. & Yuan, C. 2008 Effect of activated carbon fiber anode structure and electrolysis conditions on electrochemical degradation of dye wastewater. *J. Hazard. Mater.* **157** (1), 79–87.

Zhao, J., Zhu, C., Lu, J., Hu, C., Peng, S. & Chen, T. 2014 Electro-catalytic degradation of bisphenol A with modified Co_3O_4/β-PbO_2/Ti electrode. *Electrochim. Acta* **118** (3), 169–175.

Zhu, X., Ni, J., Li, H., Jiang, Y., Xing, X. & Borthwick, A. G. L. 2010 Effects of ultrasound on electrochemical oxidation mechanisms of *p*-substituted phenols at BDD and PbO_2 anodes. *Electrochim. Acta* **55** (20), 5569–5575.

Zhuo, Q., Deng, S., Yang, B., Huang, J. & Yu, G. 2011 Efficient electrochemical oxidation of perfluorooctanoate using Ti/SnO_2-Sb-Bi anode. *Environ. Sci. Technol.* **45** (7), 2973–2979.

First received 8 September 2015; accepted in revised form 12 November 2015. Available online 4 January 2016